

---

# Just Functioning as a Hook for Two-Stage Referring Multi-Object Tracking

---

Weize Li

Yunhao Du

Qixiang Yin

Zhicheng Zhao

Fei Su

Daqi Liu

## Abstract

Referring Multi-Object Tracking (RMOT) aims to localize target trajectories specified by natural language expressions in videos. Existing RMOT methods mainly follow two paradigms: one-stage strategies and two-stage ones. The former jointly trains tracking with referring but suffers from substantial computational overhead. Although the latter improves efficiency, it overlooks the inherent contextual aggregation capabilities of pre-trained visual backbones and takes a detour. Meanwhile, its fixed dual-tower architecture restricts compatibility with other visual / text backbones. To address these limitations, we propose JustHook, a novel hook-like framework for two-stage RMOT, which introduces two core components: (1) a Visual Feature Hook (VFH), enabling JustHook to extract context-rich local features directly from the original visual backbone like a hook; (2) a Parallel Combined Decoder (PCD), which transforms the passive cosine similarity measurement between independent modalities into active contrastive learning within the combined feature space. The proposed JustHook not only leverages the capabilities of pre-trained models but also breaks free from the constraints of inherent modality alignment, achieving strong scalability. Extensive experiments on Refer-KITTI and Refer-KITTI-V2 demonstrate that JustHook outperforms state-of-the-art methods across diverse encoder combinations, achieving a notable 7.77% HOTA improvement on Refer-KITTI-V2. Code will be made available soon.

## 1 Introduction

Unlike traditional cross-modal tasks such as image-text matching / retrieval [1; 2; 3], Referring Multi-Object Tracking (RMOT) [4] establishes dynamic correspondence between textual descriptions and spatiotemporal trajectories of one or multiple unique targets in video sequences. In RMOT, the tracker is required not only to establish a correspondence between the expressions and the objects, but also to track these objects throughout the video. For instance, given an expression like “black car on the left”, the model is required to provide the trajectories of all black cars on the left side of the video while filtering out semantically irrelevant objects. The introduction of natural language makes RMOT require both a fine-grained understanding of the specific attributes (like color) and the grasp of targets’ contextual information (like location) within the entire video.

Existing RMOT methods mainly follow two architectural paradigms: one-stage and two-stage. Current one-stage methods [4; 5; 6] connect the tracker and the matcher in series through soft decoupling, which introduce auxiliary classification modules after the conventional MOT architecture MOTR [7] to verify the correspondence between expressions and targets. Although they enable end-to-end referring tracking, the relatively high computational overhead of MOTR prevents their widespread application in practical scenarios. In contrast, two-stage methods [8] adopt hard decoupling by developing specialized cross-modal matchers that operate on trajectory proposals generated by off-

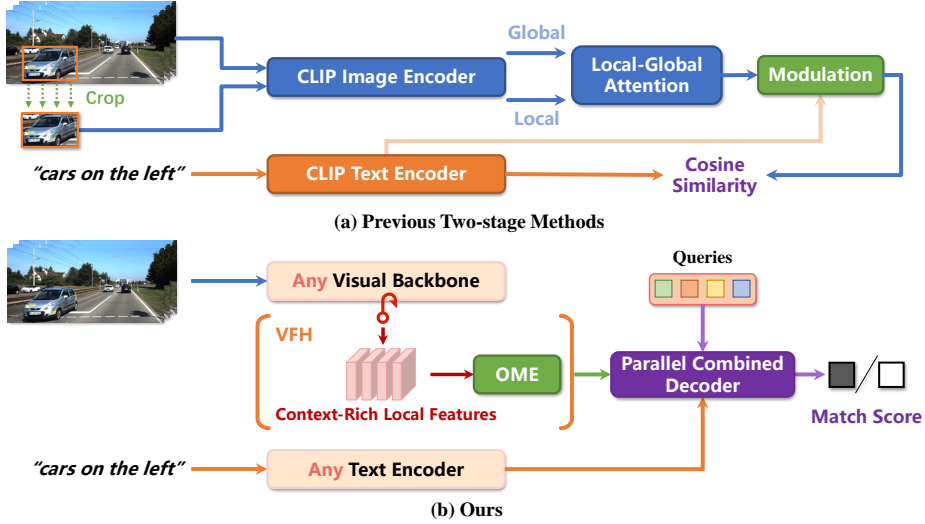


Figure 1: The comparison between previous two-stage RMOT frameworks and ours. (a) illustrates existing two-stage methods, which utilize the CLIP visual-textual feature space and feed both global and cropped images into the image encoder to enhance the contextual information. (b) presents the proposed JustHook, which operates like a hook to directly extract context-rich local features from any visual backbone without the need for additional modules or reusing the backbone.

the-shelf trackers. This modular design inherently provides greater flexibility in tracker selection and scalability across diverse scenarios.

However, in their pursuit of architectural decoupling from trackers, current representative two-stage methods, taking iKUN [8] as an example, actually make a detour and lack the full utilization of visual backbones. As shown in Fig. 1 (a), to meet the requirements of RMOT, iKUN reuses the CLIP image encoder to encode the global image and the cropped target image. Then, an additional local-global interaction module is introduced to extract the context-rich target visual features. Finally, to correct the semantic space offset generated during this process, it also needs to further modulate the visual features using the text features. Therefore, it inevitably damages the carefully constructed semantic space of CLIP, thus resulting in iKUN’s inability to generalize to the complex Refer-KITTI-V2 dataset (with only 10.32% HOTA and 2.17% DetA). In fact, most visual backbones (e.g., ResNet [9], Swin [10]) exhibit excellent contextual capabilities inherently through progressive (rather than abrupt) receptive field expansion. Even CLIP [1], which is pre-trained at the image level, still possesses fine-grained capabilities [11; 12].

In addition, to easily leverage the capabilities of the pre-trained CLIP, existing two-stage frameworks are directly designed based on the dual-tower structure of CLIP. As illustrated in Fig. 1 (a), their passive approach of measuring alignment between visual and text modalities via cosine similarity confines current two-stage RMOT methods to CLIP’s semantic space, while CLIP itself inherently possesses modality alignment capabilities. Such a modality-independent perspective greatly limits the integration with other advanced encoders and fails to achieve future-proofing.

To address these issues, we propose a novel hook-like framework called JustHook as shown in Fig. 1 (b). The proposed Visual Feature Hook (VFH) operates like a hook, fully preserving the original workflow of visual backbones while extracting context-rich local features without reusing the backbone. Its efficient extraction capability and fully decoupled design enable JustHook to fully unleash the performance of the pre-trained model and integrate seamlessly with various off-the-shelf visual backbones. In VFH, we design an Optical-flow-based Motion Extractor (OME) to replace iKUN’s simplistic temporal pooling to obtain more accurate motion information. Then, we further transform the previous dual-tower structure into an encoder-decoder structure. Using the proposed Parallel Combined Decoder (PCD), JustHook converts the original passive measurement between independent modalities into an active inspection within the combined feature space, making the two-stage RMOT no longer strongly dependent on the inherent semantic space of CLIP. Ultimately,

the proposed JustHook framework enables coupling with any visual backbone and any text encoder, and outperforms state-of-the-art (SOTA) methods on widely used Refer-KITTI [4] and Refer-KITTI-v2 [5] datasets. Our contributions can be summarized as follows:

- (1) We propose a novel hook-like framework called JustHook, which directly extracts context-rich local features from the original encoding process of the visual backbone without additional modules or reusing the backbone, thus more fully unleashing the knowledge in pre-trained models.
- (2) We transform current two-stage RMOT methods from modality-separated measurement into understanding and classifying sample pairs within a combined space, which eliminates the dependency on the inherent modality alignment of CLIP, thereby enhancing the performance and adaptability to new advancements.
- (3) By efficiently extracting visual features and decoding in the combined feature space, the proposed VFH and PCD modules achieve effective coupling with arbitrary encoders and obtain robust performance improvement.
- (4) JustHook outperforms state-of-the-art (SOTA) methods in both performance and efficiency on widely used RMOT datasets Refer-KITTI and Refer-KITTI-V2. It achieves a 7.77% improvement in HOTA metric and performs well across various combinations of visual / text encoders, demonstrating its superiority and robustness.

## 2 Related Work

### 2.1 Referring Single Object Tracking

Referring Single Object Tracking (RSOT) has been studied for several years. Most SOTA methods [13; 14; 15] follow classic tracking strategies, integrating advancements in referring video segmentation [16] (or detection [17]) and focusing on end-to-end joint tracking algorithms. JointVLT [18] guides the model to perform grounding in the first frame by inputting only a zero-pad, and then continuously tracks the target in subsequent frames based on template and expression. TransVLT [19] uses a set of proxy tokens for cross-modal information fusion, which project linguistic features and generate kernel vectors to modulate visual features. Instead of directly decoding the bounding boxes, MMTrack [20] constructs a set of queries from expression and bounding box cues and generates the target trajectories using an autoregressive approach. Although RSOT has made significant achievements [21; 22], its development is limited by highly limited task scenarios.

### 2.2 Referring Multi Object Tracking

TransRMOT [4] has pioneered RMOT by introducing the Refer-KITTI dataset and a baseline model based on MOTR [7]. Building on TransRMOT [4], MLS-Track [6] further designs a multi-level semantic interaction module to enhance the interaction between semantic and visual information. iKUN [8] decouples tracker and matcher, developing a modular framework that achieves superior performance compared to end-to-end baselines. Based upon recent advances, TempRMOT [5] constructs the enhanced Refer-KITTI-v2 dataset by leveraging large language models [23], achieving SOTA performance, while its computational overhead still persists. While iKUN imposes a lower training burden, its overly straightforward approach fails to effectively harness the capabilities of pre-trained models. Moreover, iKUN [8] confines existing two-stage frameworks within the CLIP [1] semantic space, rendering them non-future-proof.

## 3 Method

### 3.1 Problem Formulation

As a two-stage method, JustHook is typically integrated directly after any off-the-shelf tracker. Generally, we use a track-by-detection (TBD) tracker to maximize the efficiency advantages. Each tracked target will be matched with multiple expressions by JustHook. For a target in the current frame  $I_t$ , JustHook utilizes its trajectory over the previous  $T - 1$  frames, forming an ordered sequence of  $T$  frames:  $\{I_{t-T+1}, \dots, I_{t-1}, I_t\} \in \mathbb{R}^{T \times 3 \times H \times W}$ . Besides images, JustHook also takes the sequence of bounding box coordinates for the target in each frame as input:  $\{B_{t-T+1}, \dots, B_{t-1}, B_t\} \in \mathbb{R}^{T \times 4}$ ,

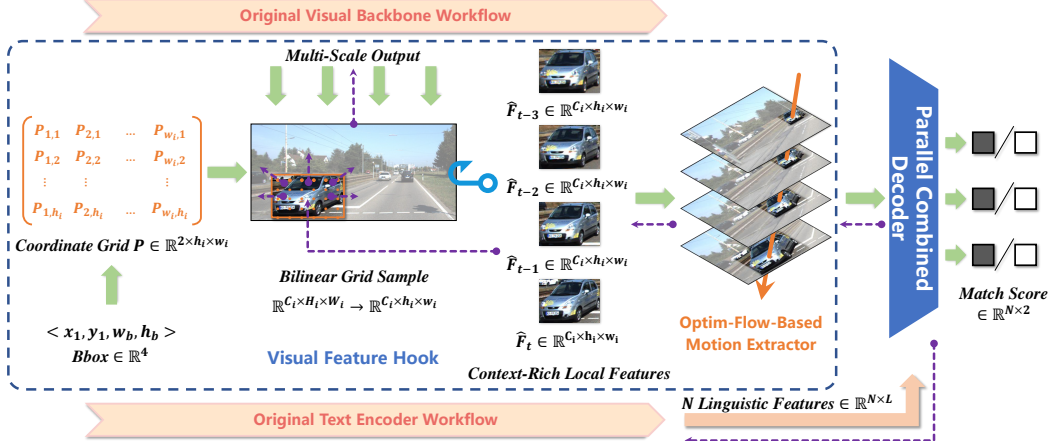


Figure 2: The overall framework of JustHook. During the encoding process of the visual backbone, JustHook directly extracts the target regions from the multi-scale visual features through grid sampling. The optical flow information constructed from these features is then aggregated into the trajectory features  $J$  after OME. Finally, the trajectory features and multiple linguistic features are decoded in parallel into multiple groups of Match Score  $O$  in PCD. The purple dotted line represents the backpropagation path of the gradient. Even though only the features of the target regions are sampled, the VFH will still propagate the gradient to other regions through visual backbone, thus adaptively obtaining the required contextual information.

which are directly derived from the tracker. At each step, a set of  $N$  expressions is sampled, and their linguistic features are extracted from the text encoder:  $\{E_1, E_2, \dots, E_N\} \in \mathbb{R}^{N \times L \times \bar{C}_t}$ , where  $L$  represents the length of the expression. Finally, JustHook outputs a set of logits  $O \in \mathbb{R}^{N \times 2}$ , where each row corresponds to the referring result between one of the  $N$  expressions and the current target.

### 3.2 A Hook-liked Framework

Hook is a mechanism in a program or system that allows for intercepting, monitoring, or modifying specific events or operations by registering callback functions to intervene in and extend certain processes [24]. As shown in Fig. 2, JustHook solves the two-stage RMOT problem by working like a Hook. Besides off-the-shelf visual backbones and text encoders, it is composed of only two parts, namely the Visual Feature Hook (VFH) and the Parallel Combined Decoder (PCD), which is simple yet effective. In the VFH, JustHook constructs a target position grid using bounding boxes and extracts target features from multi-scale visual feature maps through bilinear grid sampling. On the one hand, direct feature sampling enables VFH to efficiently extract local features that incorporate contextual information aggregated by the visual backbone. On the other hand, since bilinear grid sampling does not impede gradient propagation, VFH can leverage the gradient pathways of the backbone network to adaptively adjust the contextual information of local features. Subsequently, the Optim-Flow-Based Motion Extractor (OME) aggregates the local features from multiple frames into trajectory features. Finally, the PCD integrates bimodal features and directly decodes pair-wise matching scores within the combined feature space. Simultaneously, it processes each target against multiple texts in parallel, which not only boosts inference efficiency but also elevates performance via contrastive learning.

### 3.3 Visual Feature Hook

**Context-Rich Local Features** As shown in Fig. 3, in VFH, we first convert the input bounding box sequence  $B = \langle x_1, y_1, w_b, h_b \rangle \in \mathbb{R}^4$  into a continuous coordinate grid  $P \in \mathbb{R}^{2 \times h_i \times w_i}$ , where  $(x_1, y_1)$  represents the coordinates of the top-left corner of the target,  $w_b$  and  $h_b$  are the width and height of the bounding box, and  $w_i$  and  $h_i$  represent the width and height of the target features in the  $i$ -th layer. The elements  $P_{i,j}$  in the coordinate grid are calculated as follows:

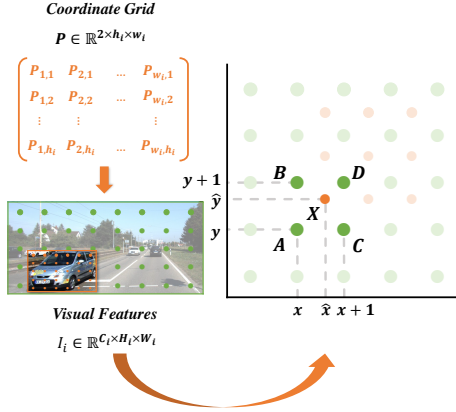


Figure 3: Illustration of bilinear grid sample. Leveraging the four nearest feature pixels and their coordinates, grid sampling can compute features at arbitrary continuous coordinates via bilinear interpolation.

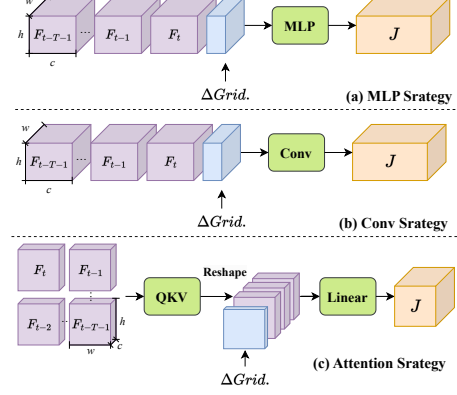


Figure 4: Three strategy of OME. (a) MLP stratagy only transforms channel, (b) Conv stratagy perceives space using convolution, and (c) Attention stratagy perceives space using self-attention.

$$\begin{aligned}
 P_{i,j} &= P_{1,1} + (i-1) \cdot \Delta x + (j-1) \cdot \Delta y \\
 \Delta x &= \left( \frac{w_b}{w_i}, 0 \right), \Delta y = \left( 0, \frac{h_b}{h_i} \right)
 \end{aligned} \tag{1}$$

where,  $P_{1,1} = (x_1, y_1)$ , and  $\Delta x$  and  $\Delta y$  represent the stride between sampling points. Taking the sampled pixel  $X \in \mathbb{R}_i^C$  as an example, its coordinate is  $P_x = (\hat{x}, \hat{y}) \in \mathbb{R}^2$ . Through the four feature pixels  $A, B, C, D$  on the original feature map that are closest to  $X$ ,  $X$  can be calculated using the following bilinear interpolation:

$$X = (1-w)(1-h)A + w(1-h)B + (1-w)hC + whD \tag{2}$$

where the coordinate of the lower-left pixel  $A$  is  $P_A = (x, y) \in \mathbb{N}^2$ . Correspondingly, the coordinate of the upper-right point  $D$  is  $P_A = (x+1, y+1) \in \mathbb{N}^2$ . And  $w = \hat{x} - x$ ,  $h = \hat{y} - y$  are respectively the offset of  $X$  in the horizontal and vertical directions relative to the point  $A$ .

Direct feature-level sampling allows VFH to efficiently harness the intrinsic contextual capabilities of pre-trained models. Meanwhile, by preserving gradient flow continuity, the grid sample ensures that although VFH only samples features from the target region, gradients can still propagate globally via the backbone network. This enables VFH to inherently acquire the contextual knowledge that has been integrated by pre-trained networks and adjust it simply by encoding the global image. It becomes particularly pronounced in dense visual backbones as well as Transformer-based backbones designed for long-range modeling.

**Optim-flow-based motion extractor** Motion information is an indispensable part of processing motion expressions (e.g., "the car turning left") in RMOT. However, the existing two-stage methods only use simple temporal pooling to compress multi-frame information, ignoring the target optical flow naturally provided by the trajectory proposals in the two-stage RMOT, which is one of the most widely used and effective methods for describing the motion information in a visual scene. Therefore, we concatenate along the channel dimension both the coordinate grid displacements  $\Delta Grid = \text{Cat}(\{P_{t-i} - P_{t-i-1}\}_{i=0}^T)$ , which serve as explicit optical flow (the blue part in Fig. 4), and the multi-frame Context-Rich Local Features, which serve as feature optical flow (the purple part in Fig. 4), thereby effectively utilizing the trajectory proposals to form target optical flow features. Meanwhile, to further enhance the model's perception capability in the spatial dimension, we design three different strategies: (1) MLP strategy, where features are simply fused using a multi-Layer perceptron (MLP); (2) Conv strategy, which applies convolution after channel-wise concatenation to

focus on the local information of the target; and (3) Attention strategy, which leverages inter-frame self-attention [25] to adaptively highlight regions of interest.

### 3.4 Parallel Combined Decoder

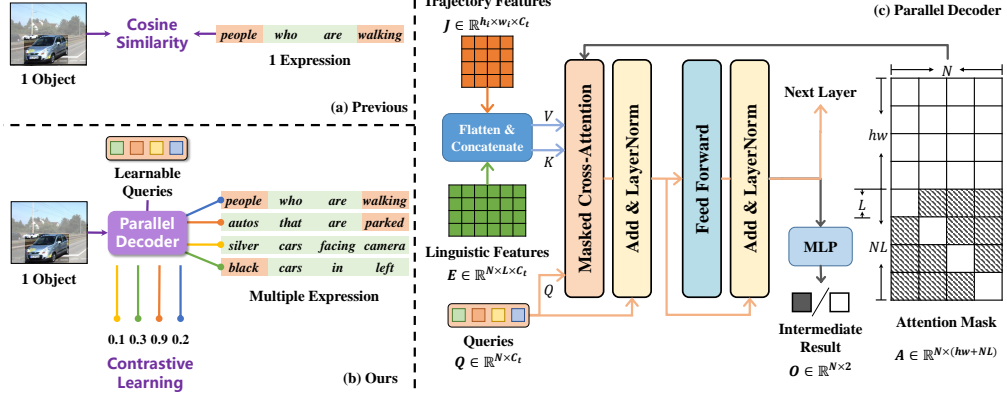


Figure 5: Illustration of the PCD. Compared with the passive strategy of cosine similarity for single sample pairs in (a), PCD actively examines the matching situations of combined sample pairs in the manner shown in (b) and conducts contrastive learning, no longer relying on the modality alignment capability inherent in CLIP. In (c), the composition of PCD is specifically introduced, which is mainly composed of mask cross-attention and FFN.

To mitigate the dependency on the modality alignment of encoders and keep future-proofing, we adopt an encoder-decoder strategy within the combined space instead of the cosine similarity-based score computation between independent modalities. As illustrated in Fig. 5 (b), the proposed Parallel Combined Decoder (PCD) operates on unified semantic representations formed by the concatenation of visual features and expression words. Rather than treating each modality separately, the PCD takes the combination of the two modalities as the basic feature space. In this way, the cross-modal matching is transformed into a task of understanding and classifying sample pairs within a combined space.

Specifically, as shown in Fig. 5 (c), after concatenating the trajectory features  $J \in \mathbb{R}^{C_t \times h_i \times w_i}$  and linguistic features  $E \in \mathbb{R}^{N \times L \times C_t}$  in the spatial dimension (the word dimension in  $E$ ), PCD uses them as Key and Value, with the learnable query vectors  $Q \in \mathbb{R}^{N \times C_t}$  as the Query, to perform masked cross-attention. The extracted information is then further summarized through a Feed-Forward Network (FFN) followed by an MLP to generate the match scores  $O \in \mathbb{R}^{N \times 2}$ . In the cross-attention mask  $A \in \mathbb{R}^{N \times (h_i \cdot w_i + N \cdot L)}$ , we assign expressions to the query vectors one by one and ensure that the visual semantics are always visible to all query vectors. At each layer, we iteratively decode queries from shallow to deep, facilitating the analysis of the target state at different feature granularity.

Through the delicate design of the attention mask, PCD further extends the previous serial processing in Fig. 5 (a) into a parallel processing paradigm for multiple expressions, which enables explicit contrastive learning between sample pairs and improves the inference efficiency. Meanwhile, compared with relying on the inherent classification hyperplane of the modality-aligned semantic spaces, the approach of actively solving the hyperplane by combining bimodal features is more suitable for pairing with various emerging encoders, liberating two-stage RMOT from the dependence on CLIP.

### 3.5 Loss Computation

We supervise all intermediate and final results using a multi-class cross-entropy loss similar to Focal Loss [36] to enhance the model’s multi-scale capability and alleviate the imbalanced sample distribution in the dataset:

$$L = - \sum_N [\alpha \cdot y_n + (1 - \alpha)(1 - y_n)] \cdot l_h \quad (3)$$

Table 1: Comparison with state-of-the-art methods on Refer-KITTI [4] and Refer-KITTI-V2 [5].

|                | Method           |                  | HOTA         | DetA         | AssA         | LocA         |
|----------------|------------------|------------------|--------------|--------------|--------------|--------------|
| Refer-KITTI    |                  |                  |              |              |              |              |
| One-Stage      | EchoTrack [26]   |                  | 39.47        | 31.19        | 51.56        | 79.93        |
|                | DeepRMOT [27]    |                  | 39.55        | 30.12        | 53.23        | 80.49        |
|                | TransRMOT [4]    |                  | 46.56        | 37.97        | 57.33        | 90.33        |
|                | MLS-Track [6]    |                  | 49.05        | 40.03        | 60.25        | -            |
|                | TempRMOT [5]     |                  | 52.21        | 40.95        | 66.75        | 90.40        |
| Two-Stage      | FairMOT [28]     |                  | 22.78        | 14.43        | 39.11        | 74.77        |
|                | DeepSORT [29]    |                  | 25.59        | 19.76        | 34.31        | 71.34        |
|                | ByteTrack [30]   |                  | 24.95        | 15.50        | 43.11        | 73.90        |
|                | CStrack [31]     |                  | 27.91        | 20.65        | 39.10        | 79.51        |
|                | TransTrack [4]   |                  | 32.77        | 23.31        | 45.71        | 79.48        |
|                | TrackFormer [32] |                  | 33.26        | 25.44        | 45.87        | 79.63        |
|                | iKUN [8]         |                  | 48.84        | 35.74        | 66.80        | -            |
|                | CLIP [1]         | CLIP-R 50 [1]    | 52.93        | 42.36        | 66.22        | 90.82        |
| JustHook       | BERT [33]        | Swin-T [10]      | 51.12        | 39.85        | 65.75        | 89.58        |
|                |                  | Resnet34 [9]     | 53.15        | 42.77        | 66.23        | 89.72        |
|                |                  | ROPE Swin-T [34] | 53.30        | 42.44        | 67.13        | 89.46        |
|                | RoBERTa [35]     | Swin-T [10]      | 51.03        | 39.50        | 65.99        | <b>90.98</b> |
|                |                  | Resnet34 [9]     | 53.28        | 41.89        | <b>67.87</b> | 90.75        |
|                |                  | ROPE Swin-T [34] | <b>53.83</b> | <b>43.40</b> | 66.86        | 90.85        |
| Refer-KITTI-V2 |                  |                  |              |              |              |              |
| One-Stage      | TransRMOT [4]    |                  | 31.00        | 19.40        | 49.68        | 89.82        |
|                | TempRMOT [5]     |                  | 35.04        | 22.97        | 53.58        | <b>90.07</b> |
| Two-Stage      | FairMOT [28]     |                  | 22.53        | 15.80        | 32.82        | 78.28        |
|                | ByteTrack [30]   |                  | 24.59        | 16.78        | 36.63        | 78.00        |
|                | iKUN [8]         |                  | 10.32        | 2.17         | 49.77        | 74.56        |
|                | JustHook         | CLIP [1]         | 41.44        | 28.71        | <b>59.95</b> | 89.12        |
|                |                  | BERT [33]        | Swin-T [10]  | 41.14        | 28.78        | 58.94        |
|                |                  |                  | Resnet34 [9] | 41.04        | 29.24        | 57.76        |
|                | RoBERTa [35]     | ROPE Swin-T [34] | 41.16        | 29.41        | 57.76        | 89.52        |
|                |                  | Swin-T [10]      | 40.32        | 27.47        | 59.29        | 88.96        |
|                |                  |                  | Resnet34 [9] | 41.71        | 30.07        | 57.99        |
|                |                  |                  | <b>42.81</b> | <b>31.35</b> | 58.61        | 89.22        |

where,  $\alpha$  is used to balance recall and precision, while  $l_h$  is used for hard sample mining, and its calculation is as follows:

$$l_h = l_{ce} \cdot \text{detach}(h_n^\beta), \quad h_n = - \sum_{c=1}^C p(O_{n,c}) \log p(O_{n,c}) \quad (4)$$

where,  $h_n$  is the information entropy of prediction and  $\beta$  is used to control its strength. `detach` refers to the “`detach`” operation in PyTorch, which removes  $h_n$  from the computation graph to prevent it from affecting the back-propagation.

## 4 Experiment

### 4.1 Experiment Setup

**Dataset and Metrics** We report the performance of JustHook on the only two widely used datasets: Refer-KITTI [4] and Refer-KITTI-V2 [5] in the manuscript, and on Refer-Dance [8] in E.1. For Refer-KITTI, we use a small subset of labels from Refer-KITTI-V2 to correct the original annotations. We further discuss it in the Appendix. For a fair comparison, we use Higher Order Tracking

Accuracy [37] (HOA) as the main metric, following TransRMOT [4]. HOA comprehensively considers the detection and association capabilities of the tracking model. We also report the localization accuracy (LocA), the detection accuracy (DetA) and the association accuracy (AssA).

**Implement Details** Benefited from the hook-like framework, JustHook can function as a plug-and-play model that connects with any visual backbone and text encoder. The visual backbones we used include ResNet [9], Swin [10; 38], and RoPE Swin [34], all of which use the pre-trained parameters on ImageNet [39], with an input size of  $224 \times 672$  to align as closely as possible with the aspect ratio of KITTI [40]. For text encoders, we test both RoBERTa [35] and BERT [33].

In each epoch, we iterate over all frames of all targets, with sample stride 2, and each sample consists of 4 frames. During inference, the sample stride is set to 1. In each training iteration, each target is coupled with 8 randomly sampled expressions, among which 4 ones are positive and 4 ones are negative. We use AdamW [41] as the optimizer, with a learning rate of 3e-5, and train for 20 epochs. But in many cases, JustHook only requires 10 epochs to achieve good performance. All experiments are performed on two NVIDIA 4090 GPUs.

## 4.2 Benchmark Experiments

We compare our method with SOTA approaches on Refer-KITTI and Refer-KITTI-V2 in Table 1. The trackers coupled with JustHook all follow the TBD paradigm, and we report only the results for the best detector & tracker here: TempRMOT [5] & NeuralSORT [8]. As a detector, TempRMOT is trained using detection labels, where each target in each frame is treated as a new target, and it only requires 10 epochs instead of 60 [5] to converge. Structurally, it can be seen as a DeformableDETR [42] with added inter-frame interactions. We further compare and discuss the impacts of different trackers [43; 44; 8; 42] on the performance of JustHook in C.

Compared to the current SOTA method TempRMOT, our best model, JustHook + RoBERTa [35] + ROPE Swin-T [34], achieves superior performance on both Refer-KITTI and Refer-KITTI-V2. JustHook has a greater advantage on Refer-KITTI-V2, surpassing TempRMOT by 7.77%, 8.38%, and 5.03% on HOA, DetA, and AssA, respectively. JustHook particularly exhibits significant advantages in HOA and DetA, demonstrating its powerful matching capability, especially on the complex Refer-KITTI-V2 dataset. We further report the performance of JustHook on Refer-Dance in E.1.

Compared with iKUN, it can be found that JustHook with the same CLIP encoder can achieve improvements of 4.09% and 31.32% on Refer-KITTI and Refer-KITTI-V2 respectively. Since in the semantic space of CLIP, the role of cosine similarity has more advantages compared with PCD, this demonstrates that VFH can make more efficient use of the knowledge of pre-trained models compared with reusing encoders and additional modules. Meanwhile, VFH adaptively extracts local features from the original backbone, causing less disruption to the original semantic space of CLIP and being more natural compared with iKUN, enabling VFH to achieve significant performance improvements on the complex Refer-KITTI-V2 dataset.

**Qualitative Results** The qualitative results can be found in F.

## 4.3 Ablation Study

**Optim-flow-based Motion Extractor** As shown in Table 3, it seems that more complex aggregation methods perform even worse than the simple MLP-based approach. This can be attributed to the fact that pre-trained visual backbones already encode rich static information within each frame. Complex aggregation strategies can distort the feature space, making subsequent learning more difficult.

**Parallel Combined Decoder** In Table 2, we investigate the performance of PCD. Among them, "Cosine Similarity" means removing PCD and instead using only the cosine similarity between the trajectory features and the textual features as the matching score. In addition, for comparison, we emulate the approach in one-stage methods by designing two Transformer-based decoding structures. They respectively represent pre-compressing visual features into textual features and the opposite process. Here,  $\mathbb{Q}$ ,  $\mathbb{L}$  and  $\mathbb{V}$  represent the query vectors, linguistic and visual features respectively.

It is evident that replacing PCD with cosine similarity results in a significant performance drop, which indicates that directly using cosine similarity to calculate matching scores in a non-CLIP semantic

Table 2: Comparison of the performance between various sequential decoding and PCD.

|                   | $Q_1$ | $KV_1$ | $Q_2$ | $KV_2$       | HOTA         | DetA         | AssA  |
|-------------------|-------|--------|-------|--------------|--------------|--------------|-------|
| #1                | V     | L      | Q     | V            | 40.85        | 29.56        | 56.59 |
| #2                | L     | V      | Q     | L            | 41.40        | 29.39        | 58.46 |
| Cosine Similarity |       |        |       | 28.29        | 13.46        | <b>59.58</b> |       |
| PCD               |       |        |       | <b>42.81</b> | <b>31.35</b> | 58.61        |       |

Table 3: Comparison of different spatial perception strategies in OME.

| Strategy  | HOTA         | DetA         | AssA         |
|-----------|--------------|--------------|--------------|
| Attention | 41.38        | 29.76        | 57.69        |
| Conv      | 41.90        | 29.79        | <b>59.06</b> |
| MLP       | <b>42.81</b> | <b>31.35</b> | 58.61        |

space can easily lead to model collapse and failure to converge. The improvement obtained on AssA by its judging all sample pairs as positive examples also proves it. Additionally, when comparing #1 and #2, it can be observed that integrating sparse visual semantics into the dense textual space achieves superior performance compared to using the visual space as the base space. However, regardless of how the order of cross-attention interactions is arranged, sequential decoding is still based on the concept of an independent modal space, and it consistently performs worse than the PCD that conducts decoding in the combined feature space.

Table 4: Impact of parameter in the loss function.

| $\alpha$   | $\beta$  | HOTA         | DetA         | AssA         |
|------------|----------|--------------|--------------|--------------|
| 0.3        | 1        | 40.11        | 29.50        | 54.72        |
| 0.5        | 1        | 41.03        | 29.68        | 56.86        |
| <b>0.7</b> | <b>1</b> | <b>42.81</b> | <b>31.35</b> | 58.61        |
| 0.9        | 1        | 41.27        | 28.58        | <b>59.72</b> |
| 0.7        | 0        | 41.25        | 29.08        | 58.64        |
| 0.7        | 2        | 41.96        | 30.61        | 57.67        |

Table 5: Comparison of training and inference time. All experiments are conducted on Refer-KITTI-V2 [5]. “ $\dagger$ ”: The overhead when training TempRMOT only for the detection task. “ $\ddagger$ ”: iKUN [8] trains at the trajectory level.

| Method                 | Epoch | Train  | Inference | HOTA  |
|------------------------|-------|--------|-----------|-------|
| TempRMOT [5]           | 50    | 62 h   | 299 min   | 35.04 |
| TempRMOT $\dagger$ [5] | 10    | 12.4 h | 2.99 min  | -     |
| iKUN $\ddagger$ [8]    | 100   | 2.51 h | 115 min   | 10.32 |
| JustHook               | 20    | 2.17 h | 27 min    | 42.82 |

**Loss Parameter** In Table 4, we evaluate the effects of different values of  $\alpha$  and  $\beta$ , which are used to balance recall and precision and control the weighting strength of hard samples, respectively.  $\alpha$  performs better when it is greater than 0.5, but when it is too high, the performance starts to degrade. Therefore, we select 0.7 as the optimal value for  $\alpha$ . When  $\alpha$  is fixed at 0.7, we vary the value of  $\beta$ . It can be observed that the weight for hard samples should neither be absent ( $\beta = 0$ ) nor excessive. The highest HOTA is achieved when  $\beta$  is set to 1.

**Training and inference time** Table 5 shows a comparison of training and inference time on our machine, where the combination of JustHook is RoBERTa [35] + ROPE Swin-T [34]. Both iKUN and TempRMOT follow the official configuration. Since iKUN only samples 4 frames of each trajectory for training in each epoch, the total epochs for iKUN are significantly high. When training TempRMOT for detection, as the dataset has only two “expressions” (car and pedestrian), TempRMOT can converge within fewer than 10 epochs. When using other detectors such as Deformable-DETR [42], the speed is generally faster. Considering that the overhead of most TBD trackers is very low, even when adding the time for training the first stage, JustHook still demonstrates a significant efficiency advantage.

More ablation experiments can be found in E

## 5 Conclusion

In this work, we address the limitations of existing two-stage RMOT methods by proposing JustHook, a flexible and efficient hook-like framework. JustHook introduces two novel components, VFH and PCD, which enable context-aware feature aggregation and parallel decoding in a combined space, achieving significant gains in accuracy and computational efficiency. By functioning like a hook, JustHook efficiently leverages the inherent contextual aggregation capabilities of pre-trained models and introduces a novel encoder-decoder architecture for the two-stage RMOT, demonstrating strong adaptability to various emerging visual/text encoders and ensuring future-proofing.

## References

- [1] Radford, A., J. W. Kim, C. Hallacy, et al. Learning transferable visual models from natural language supervision. In M. Meila, T. Zhang, eds., *Proceedings of the 38th International Conference on Machine Learning*, vol. 139 of *Proceedings of Machine Learning Research*, pages 8748–8763. PMLR, 2021.
- [2] Li, J., R. Selvaraju, A. Gotmare, et al. Align before fuse: Vision and language representation learning with momentum distillation. In M. Ranzato, A. Beygelzimer, Y. Dauphin, P. Liang, J. W. Vaughan, eds., *Advances in Neural Information Processing Systems*, vol. 34, pages 9694–9705. Curran Associates, Inc., 2021.
- [3] Schuhmann, C., R. Vencu, R. Beaumont, et al. Laion-400m: Open dataset of clip-filtered 400 million image-text pairs, 2021.
- [4] Wu, D., W. Han, T. Wang, et al. Referring multi-object tracking. In *Proceedings of the IEEE/CVF Conference on Computer Vision and Pattern Recognition (CVPR)*, pages 14633–14642. 2023.
- [5] Zhang, Y., D. Wu, W. Han, et al. Bootstrapping referring multi-object tracking, 2024.
- [6] Ma, Z., S. Yang, Z. Cui, et al. Mls-track: Multilevel semantic interaction in rmot, 2024.
- [7] Zeng, F., B. Dong, Y. Zhang, et al. Motr: End-to-end multiple-object tracking with transformer. In S. Avidan, G. Brostow, M. Cissé, G. M. Farinella, T. Hassner, eds., *Computer Vision – ECCV 2022*, pages 659–675. Springer Nature Switzerland, Cham, 2022.
- [8] Du, Y., C. Lei, Z. Zhao, et al. ikun: Speak to trackers without retraining. In *Proceedings of the IEEE/CVF Conference on Computer Vision and Pattern Recognition (CVPR)*, pages 19135–19144. 2024.
- [9] He, K., X. Zhang, S. Ren, et al. Deep residual learning for image recognition. In *Proceedings of the IEEE Conference on Computer Vision and Pattern Recognition (CVPR)*. 2016.
- [10] Liu, Z., Y. Lin, Y. Cao, et al. Swin transformer: Hierarchical vision transformer using shifted windows. In *Proceedings of the IEEE/CVF International Conference on Computer Vision (ICCV)*, pages 10012–10022. 2021.
- [11] Wang, F., J. Mei, A. Yuille. Sclip: Rethinking self-attention for dense vision-language inference. In A. Leonardis, E. Ricci, S. Roth, O. Russakovsky, T. Sattler, G. Varol, eds., *Computer Vision – ECCV 2024*, pages 315–332. Springer Nature Switzerland, Cham, 2025.
- [12] Lan, M., C. Chen, Y. Ke, et al. Clearclip: Decomposing clip representations for dense vision-language inference. In A. Leonardis, E. Ricci, S. Roth, O. Russakovsky, T. Sattler, G. Varol, eds., *Computer Vision – ECCV 2024*, pages 143–160. Springer Nature Switzerland, Cham, 2025.
- [13] Botach, A., E. Zheltonozhskii, C. Baskin. End-to-end referring video object segmentation with multimodal transformers. In *Proceedings of the IEEE/CVF Conference on Computer Vision and Pattern Recognition (CVPR)*, pages 4985–4995. 2022.
- [14] Wu, J., Y. Jiang, P. Sun, et al. Language as queries for referring video object segmentation. In *Proceedings of the IEEE/CVF Conference on Computer Vision and Pattern Recognition (CVPR)*, pages 4974–4984. 2022.
- [15] Wu, D., T. Wang, Y. Zhang, et al. Onlinerefer: A simple online baseline for referring video object segmentation. In *Proceedings of the IEEE/CVF International Conference on Computer Vision (ICCV)*, pages 2761–2770. 2023.
- [16] Ding, H., C. Liu, S. He, et al. Mevis: A large-scale benchmark for video segmentation with motion expressions. In *Proceedings of the IEEE/CVF International Conference on Computer Vision (ICCV)*, pages 2694–2703. 2023.
- [17] Wen, L., D. Du, Z. Cai, et al. Ua-detrac: A new benchmark and protocol for multi-object detection and tracking. *Computer Vision and Image Understanding*, 193:102907, 2020.
- [18] Zhao, H., X. Wang, D. Wang, et al. Transformer vision-language tracking via proxy token guided cross-modal fusion. *Pattern Recognition Letters*, 168:10–16, 2023.
- [19] Zhou, L., Z. Zhou, K. Mao, et al. Joint visual grounding and tracking with natural language specification. In *Proceedings of the IEEE/CVF Conference on Computer Vision and Pattern Recognition (CVPR)*, pages 23151–23160. 2023.

[20] Zheng, Y., B. Zhong, Q. Liang, et al. Toward unified token learning for vision-language tracking. *IEEE Transactions on Circuits and Systems for Video Technology*, 34(4):2125–2135, 2024.

[21] Kang, B., X. Chen, S. Lai, et al. Exploring enhanced contextual information for video-level object tracking. In *AAAI*. 2025.

[22] Zhang, H., J. Wang, J. Zhang, et al. One-stream vision-language memory network for object tracking. *IEEE Transactions on Multimedia*, 26:1720–1730, 2024.

[23] Brown, T., B. Mann, N. Ryder, et al. Language models are few-shot learners. In H. Larochelle, M. Ranzato, R. Hadsell, M. Balcan, H. Lin, eds., *Advances in Neural Information Processing Systems*, vol. 33, pages 1877–1901. Curran Associates, Inc., 2020.

[24] Lopez, J., L. Babun, H. Aksu, et al. A survey on function and system call hooking approaches. *Journal of Hardware and Systems Security*, 1:114–136, 2017.

[25] Vaswani, A., N. Shazeer, N. Parmar, et al. Attention is all you need. In I. Guyon, U. V. Luxburg, S. Bengio, H. Wallach, R. Fergus, S. Vishwanathan, R. Garnett, eds., *Advances in Neural Information Processing Systems*, vol. 30. Curran Associates, Inc., 2017.

[26] Lin, J., J. Chen, K. Peng, et al. Echotrack: Auditory referring multi-object tracking for autonomous driving. *IEEE Transactions on Intelligent Transportation Systems*, 25(11):18964–18977, 2024.

[27] He, W., Y. Jian, Y. Lu, et al. Visual-linguistic representation learning with deep cross-modality fusion for referring multi-object tracking. In *ICASSP 2024 - 2024 IEEE International Conference on Acoustics, Speech and Signal Processing (ICASSP)*, pages 6310–6314. 2024.

[28] Zhang, Y., C. Wang, X. Wang, et al. Fairmot: On the fairness of detection and re-identification in multiple object tracking. *International journal of computer vision*, 129:3069–3087, 2021.

[29] Wojke, N., A. Bewley, D. Paulus. Simple online and realtime tracking with a deep association metric. In *2017 IEEE International Conference on Image Processing (ICIP)*, pages 3645–3649. 2017.

[30] Zhang, Y., P. Sun, Y. Jiang, et al. Bytetrack: Multi-object tracking by associating every detection box. In S. Avidan, G. Brostow, M. Cissé, G. M. Farinella, T. Hassner, eds., *Computer Vision – ECCV 2022*, pages 1–21. Springer Nature Switzerland, Cham, 2022.

[31] Liang, C., Z. Zhang, X. Zhou, et al. Rethinking the competition between detection and reid in multiobject tracking. *IEEE Transactions on Image Processing*, 31:3182–3196, 2022.

[32] Meinhardt, T., A. Kirillov, L. Leal-Taixé, et al. Trackformer: Multi-object tracking with transformers. In *Proceedings of the IEEE/CVF Conference on Computer Vision and Pattern Recognition (CVPR)*, pages 8844–8854. 2022.

[33] Devlin, J., M.-W. Chang, K. Lee, et al. BERT: Pre-training of deep bidirectional transformers for language understanding. In J. Burstein, C. Doran, T. Solorio, eds., *Proceedings of the 2019 Conference of the North American Chapter of the Association for Computational Linguistics: Human Language Technologies, Volume 1 (Long and Short Papers)*, pages 4171–4186. Association for Computational Linguistics, Minneapolis, Minnesota, 2019.

[34] Heo, B., S. Park, D. Han, et al. Rotary position embedding for vision transformer. In *European Conference on Computer Vision (ECCV)*. 2024.

[35] Liu, Y., M. Ott, N. Goyal, et al. Roberta: A robustly optimized bert pretraining approach, 2019.

[36] Lin, T.-Y., P. Goyal, R. Girshick, et al. Focal loss for dense object detection. In *Proceedings of the IEEE International Conference on Computer Vision (ICCV)*. 2017.

[37] Luiten, J., A. Osep, P. Dendorfer, et al. Hota: A higher order metric for evaluating multi-object tracking. *International journal of computer vision*, 129:548–578, 2021.

[38] Liu, Z., H. Hu, Y. Lin, et al. Swin transformer v2: Scaling up capacity and resolution. In *Proceedings of the IEEE/CVF Conference on Computer Vision and Pattern Recognition (CVPR)*, pages 12009–12019. 2022.

[39] Deng, J., W. Dong, R. Socher, et al. Imagenet: A large-scale hierarchical image database. In *2009 IEEE Conference on Computer Vision and Pattern Recognition*, pages 248–255. 2009.

[40] Geiger, A., P. Lenz, R. Urtasun. Are we ready for autonomous driving? the kitti vision benchmark suite. In *2012 IEEE Conference on Computer Vision and Pattern Recognition*, pages 3354–3361. 2012.

- [41] Loshchilov, I., F. Hutter. Decoupled weight decay regularization, 2019.
- [42] Zhu, X., W. Su, L. Lu, et al. Deformable detr: Deformable transformers for end-to-end object detection, 2021.
- [43] Cao, J., J. Pang, X. Weng, et al. Observation-centric sort: Rethinking sort for robust multi-object tracking. In *Proceedings of the IEEE/CVF Conference on Computer Vision and Pattern Recognition (CVPR)*, pages 9686–9696. 2023.
- [44] Du, Y., Z. Zhao, Y. Song, et al. Strongsort: Make deepsort great again. *IEEE Transactions on Multimedia*, 25:8725–8737, 2023.

## A Dataset Details

### A.1 Refer-KITTI

Refer-KITTI [14] uses 18 low-complexity videos and tracking annotations from the KITTI [40] training set, encompassing a total of 895 expressions [5]. During the annotation process, manual bidirectional verification is performed on the matching between expressions and targets to ensure annotation accuracy. Although Refer-KITTI lays the foundation for RMOT, its test set is relatively small and exhibits a significant distribution gap from the training set, resulting in a failure to accurately reflect real-world scenarios [5].

### A.2 Refer-KITTI-V2

Recognizing the issues in Refer-KITTI, Refer-KITTI-V2 [5] leverages large language models to further enrich the diversity of expressions in Refer-KITTI. Building on the 18 videos from Refer-KITTI, Refer-KITTI-V2 includes 9758 expressions and an additional 3 videos from the KITTI [40] training set, with 2 used for training and 1 for testing. The diversified expressions and more complex scenarios make Refer-KITTI-V2 more reflective of real-world conditions compared to Refer-KITTI, presenting new challenges for RMOT.

### A.3 Correction for Refer-KITTI

Refer-KITTI has suffered from multiple annotation errors for a long time. Many critical issues such as frame misalignment have been addressed in iKUN [8] and Refer-KITTI-V2 [5]. However, the problem of incomplete reference persists in the current version. For instance, in frames 231-232 of video “0002”, two silver vehicles are referenced under the label “left cars in light color” but are missing in the “left cars in silver”. In addition to these general errors, there are also some special errors in Refer-KITTI, and the impacts they have on one-stage methods and two-stage methods are inherently inconsistent. That is, numerous objects originally annotated in the tracking annotations of Refer-KITTI are entirely omitted in referring annotations of Refer-KITTI, such as all pedestrians in video “0001”. Because one-stage methods use all tracking annotations for training while two-stage methods are only based on referring annotations, this issue leads to particularly significant adverse effects on two-stage methods.

Table 6: Performance comparison of TempRMOT [5] before and after the correction of Refer-KITTI [4].

| Correction | HOTA  | DetA  | AssA  |
|------------|-------|-------|-------|
| Before     | 52.21 | 40.95 | 66.75 |
| After      | 51.79 | 40.28 | 66.68 |

Therefore, for a fair comparison, we select expressions from Refer-KITTI-V2 that consist solely of words previously used in Refer-KITTI and replace the original annotations with them. Due to the complete referencing of these missing targets in Refer-KITTI-v2, this approach resolves the existing issues in Refer-KITTI without introducing new words or causing data leakage. To verify the rationality of our correction strategy, we retrain TempRMOT [5] using the corrected Refer-KITTI dataset. As shown in Table 6, our correction strategy does not affect the one-stage methods, since TempRMOT itself already utilizes all the tracking annotations.

## B Limitations

Many experiments show that JustHook has a significantly greater gain on Refer-KITTI-V2 than on Refer-KITTI. On the one hand, it can be attributed to the fact that the Refer-KITTI dataset is simpler, with less data and relatively simple text, leaving limited room for improvement. This can be verified in Table 7. Without considering the expressions at all, the pure multi-object tracking performance on Refer-KITTI is only 63.7% HOTA, while the HOTA of over 50 on RMOT nowadays is already very close to this theoretical upper limit. On the other hand, as a two-stage method, JustHook is fundamentally based on solving the classification hyperplane in the combined feature space. This means that compared with one-stage methods, two-stage methods generally have higher requirements for the amount of data and its diversity. Larger quantities of more complex training data are often helpful in providing more support vectors to assist in determining the classification hyperplane. Therefore, JustHook shows a more obvious improvement in performance on the complex dataset Refer-KITTI-v2 and is also more suitable for practical applications in complex real-world scenarios. In the future, through methods such as data augmentation and synthesis, exploring the work of mining difficult samples will be more conducive to the development of two-stage RMOT.

## C Discussion and Performance of other Trackers

Table 7: Performance comparison of multi-object tracking on KITTI [40] (using the same split as Refer-KITTI-v2 [5]). “ $\dagger$ ” and “ $\ddagger$ ” denote the tracker and detector versions of TempRMOT [5], respectively.

|           | Detector            | Tracker         | HOTA         | DetA         | AssA         | LocA         |
|-----------|---------------------|-----------------|--------------|--------------|--------------|--------------|
| One-stage | TempRMOT $\dagger$  |                 | <b>63.47</b> | 56.09        | <b>72.04</b> | <b>91.19</b> |
| Two-stage | D-DETR [42]         | OC-SORT [43]    | 54.13        | 50.31        | 58.46        | 90.73        |
|           |                     | StrongSORT [44] | 56.98        | 54.13        | 60.20        | 90.24        |
|           |                     | NeuralSORT [8]  | 56.84        | 54.37        | 59.67        | 89.89        |
|           | TempRMOT $\ddagger$ | OC-SORT [43]    | 58.26        | 55.35        | 61.57        | 90.44        |
|           |                     | StrongSORT [44] | 59.42        | 57.25        | 61.92        | 89.91        |
|           |                     | NeuralSORT [8]  | 61.10        | <b>57.56</b> | 65.08        | 89.84        |

As a two-stage RMOT method, the proposed JustHook can be coupled with arbitrary trackers, achieving seamless integration with any tracker, any visual backbone, and any text encoder. In order to better illustrate that the gains generated by JustHook compared with the current SOTA method TempRMOT [5] do not stem from the improvement of the tracker’s performance, in Table 7, we compare the pure multi-object tracking performance of different detector/tracker combinations (for TBD paradigm) employed in our approach with that of TempRMOT $\dagger$  (as a pure one-stage MOT model). Here, “D-DETR” refers to DeformableDETR [42]. In the two-stage (TBD) method, TempRMOT $\ddagger$  serves solely as a detector and adheres to the detection paradigm, where we treat each target in each frame as a new addition. Combined with the comparison of RMOT capabilities in Table 1, it can be seen that even trackers with weaker tracking capabilities than TempRMOT $\dagger$  can achieve performance exceeding the SOTA method TempRMOT [5] in RMOT after integrating JustHook. This demonstrates that JustHook significantly surpasses TempRMOT in matching capability, providing excellent results even when coupled with inferior trackers.

Furthermore, we compare the performance changes of JustHook on RMOT after replacing these TBD-style trackers in Table 8. JustHook achieves consistent performance improvements as the capability of the detectors / trackers increases, highlighting its flexibility and robustness.

## D Broader Impact

JustHook further propels the research of RMOT, which enriches the technical means of computer vision by using language expressions as semantic cues to guide multi-object tracking predictions. This is of great significance for the development of related industries such as autonomous driving, which can improve the environmental perception ability of autonomous vehicles and enhance the safety and reliability of driving.

Table 8: Performance comparison of JustHook coupled with different trackers, visual backbones, and text encoders on Refer-KITTI-V2 [5].

| Detector & Tracker             | Text Encoder | Visual Backbone  | HOTA         | DetA         | AssA         | LocA         |
|--------------------------------|--------------|------------------|--------------|--------------|--------------|--------------|
|                                | TempRMOT [5] |                  | 35.04        | 22.97        | 53.58        | 90.07        |
| D-DETR [42] & OC-SORT [43]     | BERT [33]    | Swin-T [10]      | 37.56        | 27.43        | 51.58        | 89.70        |
|                                |              | Resnet34 [9]     | 37.83        | 27.95        | 51.36        | 89.92        |
|                                |              | ROPE Swin-T [34] | 37.91        | 27.57        | 52.28        | <b>90.28</b> |
|                                | RoBERTa [35] | Swin-T [10]      | 37.38        | 26.84        | 52.20        | 89.73        |
|                                |              | Resnet34 [9]     | 38.05        | 28.22        | 51.45        | 89.96        |
|                                |              | ROPE Swin-T [34] | 38.74        | 29.08        | 51.77        | 89.97        |
| D-DETR [42] & StrongSORT [44]  | BERT [33]    | Swin-T [10]      | 39.28        | 28.50        | 54.27        | 89.31        |
|                                |              | Resnet34 [9]     | 38.44        | 28.43        | 52.12        | 89.89        |
|                                |              | ROPE Swin-T [34] | 38.13        | 28.01        | 52.03        | 90.23        |
|                                | RoBERTa [35] | Swin-T [10]      | 38.95        | 27.73        | 54.83        | 89.32        |
|                                |              | Resnet34 [9]     | 38.60        | 28.72        | 52.03        | 89.92        |
|                                |              | ROPE Swin-T [34] | 39.26        | 29.63        | 52.16        | 89.93        |
| D-DETR [42] & NeuralSORT [8]   | BERT [33]    | Swin-T [10]      | 38.88        | 28.31        | 53.58        | 88.94        |
|                                |              | Resnet34 [9]     | 39.27        | 28.83        | 53.65        | 89.26        |
|                                |              | ROPE Swin-T [34] | 39.27        | 28.61        | 54.07        | 89.58        |
|                                | RoBERTa [35] | Swin-T [10]      | 38.58        | 27.51        | 54.27        | 88.95        |
|                                |              | Resnet34 [9]     | 39.63        | 29.38        | 53.61        | 89.24        |
|                                |              | ROPE Swin-T [34] | 40.10        | 30.30        | 53.25        | 89.17        |
| TempRMOT [5] & OC-SORT [43]    | BERT [33]    | Swin-T [10]      | 39.01        | 28.62        | 53.36        | 89.44        |
|                                |              | Resnet34 [9]     | 39.15        | 28.97        | 53.10        | 89.66        |
|                                |              | ROPE Swin-T [34] | 39.45        | 29.04        | 53.75        | 90.01        |
|                                | RoBERTa [35] | Swin-T [10]      | 38.32        | 27.49        | 53.58        | 89.45        |
|                                |              | Resnet34 [9]     | 39.81        | 29.67        | 53.58        | 89.69        |
|                                |              | ROPE Swin-T [34] | 40.56        | 30.80        | 53.59        | 89.69        |
| TempRMOT [5] & StrongSORT [44] | BERT [33]    | Swin-T [10]      | 40.54        | 28.83        | 57.18        | 89.07        |
|                                |              | Resnet34 [9]     | 40.02        | 29.16        | 55.09        | 89.64        |
|                                |              | ROPE Swin-T [34] | 39.98        | 29.16        | 54.98        | 90.01        |
|                                | RoBERTa [35] | Swin-T [10]      | 39.77        | 27.53        | 57.58        | 89.08        |
|                                |              | Resnet34 [9]     | 40.58        | 29.83        | 55.34        | 89.69        |
|                                |              | ROPE Swin-T [34] | 41.51        | 31.02        | 55.70        | 89.68        |
| TempRMOT [5] & NeuralSORT [8]  | BERT [33]    | Swin-T [10]      | 41.14        | 28.78        | 58.94        | 88.97        |
|                                |              | Resnet34 [9]     | 41.04        | 29.24        | 57.76        | 89.19        |
|                                |              | ROPE Swin-T [34] | 41.16        | 29.41        | 57.76        | 89.52        |
|                                | RoBERTa [35] | Swin-T [10]      | 40.32        | 27.47        | <b>59.29</b> | 88.96        |
|                                |              | Resnet34 [9]     | 41.71        | 30.07        | 57.99        | 89.25        |
|                                |              | ROPE Swin-T [34] | <b>42.81</b> | <b>31.35</b> | 58.61        | 89.22        |

## E More experiments

### E.1 Performance comparison on Refer-Dance

We compare the performance of iKUN [8] and JustHook on Refer-Dance [8] in Table 9. Among them, JustHook uses the best combination of encoders, RoBERTa [35] and RoPE Swin Transformer-T [34]. The intermediate results of both the detector and the tracker use the versions officially provided by iKUN [8]. It can be seen that JustHook still exhibits significant performance advantages, indicating that by fully leveraging the capabilities of pre-trained models, JustHook can achieve robust improvements compared to existing methods in various scenarios.

Table 9: Performance comparison on Refer-Dance [8].

|           | Method               | HOTA                  | DetA                  | AssA                  |
|-----------|----------------------|-----------------------|-----------------------|-----------------------|
| One-stage | TransRMOT [4]        | 9.58                  | 4.37                  | 20.99                 |
| Two-stage | iKUN [8]<br>JustHook | 29.06<br><b>31.83</b> | 25.33<br><b>30.31</b> | 33.35<br><b>33.47</b> |

Table 10: Performance of JustHook after freezing different modules on Refer-KITTI-v2 [5].

| Method         | Visual Backbone | Text Encoder | HOTA         |              |              |
|----------------|-----------------|--------------|--------------|--------------|--------------|
|                |                 |              | DetA         | AssA         |              |
| JustHook +CLIP | Trainable       | Frozen       | 40.76        | 28.93        | 57.57        |
|                | Frozen          | Trainable    | 41.17        | <b>29.48</b> | 57.65        |
|                | Frozen          | Frozen       | 40.92        | 29.07        | 57.75        |
|                | Trainable       | Trainable    | <b>41.44</b> | 28.71        | <b>59.95</b> |
| JustHook +Best | Trainable       | Frozen       | 40.44        | 28.09        | 58.38        |
|                | Frozen          | Trainable    | 41.05        | 29.73        | 56.81        |
|                | Frozen          | Frozen       | 40.55        | 28.60        | 57.62        |
|                | Trainable       | Trainable    | <b>42.81</b> | <b>31.35</b> | <b>58.61</b> |

## E.2 Impact of VFH and Freezing

In Table 10, we evaluate the impact of freezing different components in JustHook, where JustHook+CLIP represents the CLIP-R 50 [1] encoder pair, and JustHook+Best refers to the ROPE Swin-T [34] + RoBERTa [35] encoder pair. It is observed that freezing the text encoder has a more significant negative effect compared to freezing the visual backbone. This clearly demonstrates that VFH makes extremely good use of the capabilities of the pre-trained visual backbone. Thus, even when the visual backbone is frozen, there will be no significant performance loss. Moreover, VFH’s capacity to adaptively modulate contextual information facilitates a notable enhancement in performance once the visual backbone is unfrozen. However, the text encoder, whose semantic distribution diverges significantly from that of RMOT, struggles to discern subtle semantic distinctions among targets when its parameters are frozen. Therefore, training the text encoder becomes essential to enable PCD to derive a more discriminative combined feature space, thereby improving its overall discriminative power.

Additionally, freezing other encoders has a more pronounced negative impact compared to the CLIP encoders, indicating that CLIP’s inherent modality alignment effectively reduces the difficulty of constructing a unified semantic space. However, compared with the encoder pairs of CLIP, dense encoders like Swin exhibit a more pronounced performance advantage on RMOT, and training both visual / text encoders simultaneously to optimize the features of the two modalities bidirectionally consistently proves to be more beneficial.

## E.3 The Scalability of JustHook

In Table 11, we evaluate the performance of JustHook with different sizes of ResNet [9] and RoPE Swin Transformer-T [34] as visual backbones. The text encoder maintains RoBERTa [35]. It can be observed that as the size of the Swin Transformer increases, the performance of JustHook does not improve significantly and even decreases. However, for convolutional networks, as the size of ResNet increases, the performance of JustHook continues to improve, but this improvement stops at ResNet34. This indicates that the scalability of visual backbones of different sizes for JustHook is not significant, but CNN-based backbones slightly outperform Transformer-based ones. This can be attributed to the limited visual information of most targets in the current Refer-KITTI-V2 dataset, which does not require a very powerful visual backbone to characterize the target’s state. When the visual backbone is too powerful, the model is more prone to overfitting. Therefore, we ultimately selected ResNet34 and ROPE Swin-T for reporting.

Table 11: Comparison of JustHook performance with different-sized visual encoders on Refer-KITTI-v2 [5].

| Backbone       | Size  | HOTA         | DetA         | AssA         |
|----------------|-------|--------------|--------------|--------------|
| ROPE Swin [34] | Tiny  | <b>42.81</b> | <b>31.35</b> | <b>58.61</b> |
|                | Small | 41.50        | 28.76        | 60.05        |
|                | Base  | 41.16        | 29.43        | 57.70        |
| ResNet [9]     | 18    | 40.99        | 28.89        | 58.31        |
|                | 34    | <b>41.71</b> | <b>30.07</b> | <b>57.99</b> |
|                | 50    | 40.61        | 27.85        | 59.36        |

Table 12: Comparison of Performance between iKUN [8] and JustHook when coupled with different encoders on Refer-KITTI [4].

|          | Visual Backbone | Text Encoder | HOTA         | DetA         | AssA         |
|----------|-----------------|--------------|--------------|--------------|--------------|
| iKUN [8] | CLIP [1]        | CLIP [1]     | 48.84        | 35.74        | 66.80        |
|          | ROPE Swin [34]  | RoBERTa [35] | 29.79        | 14.73        | 60.38        |
| JustHook | CLIP [1]        | CLIP [1]     | 52.93        | 42.36        | 66.22        |
|          | ROPE Swin [34]  | RoBERTa [35] | <b>53.83</b> | <b>43.40</b> | <b>66.86</b> |

#### E.4 The adaptability comparison between iKUN and JustHook

To support our viewpoint that iKUN has a strong dependence on the semantic space of CLIP, we quantitatively measure the performance changes of iKUN after replacing the semantic space. Following the official configuration of iKUN [8], we evaluate its performance when coupled with other encoders in Table 12 to explore the adaptability of the current two-stage methods. Here, ROPE Swin [34] uses the tiny version, CLIP [1] adopts the ResNet50 version following iKUN [8]. It is evident that when using the best encoder combination in JustHook (i.e., ROPE Swin-T [34] & RoBERTa [35]), iKUN [8] fails to fully leverage the capabilities of advanced encoders, as JustHook does. When in a semantic space with misaligned modalities, the adaptability of iKUN’s modality-independent passive measurement is significantly lower than the combined space decoding in JustHook, resulting in a significant performance drop and making it difficult to converge. This indicates that iKUN heavily depends on encoder pairs with inherent feature alignment capabilities, such as CLIP [1], and struggles to integrate with emerging encoders, making it not capable of future proofing.

## F Qualitative Results



Figure 6: Visualization of some qualitative results (Part 1).

There are several typical referring results in Fig. 6. In the first expression, JustHook effectively distinguishes between light-colored and dark-colored vehicles and accurately understands the target’s location. In the second expression, despite the continuous movement of the visual capture, JustHook still accurately identifies that the vehicles on the right are stationary. The third expression is more complex, involving both the target’s location and gender. The final expression highlights JustHook’s adjustment in matching the target during movement. In the video, a group of pedestrians cross the

road, but the expression only describes pedestrians on the right side. As soon as the target reaches the center or shifts slightly to the left, JustHook cancels the match.

We visualize additional qualitative results in Fig. 7 and Fig. 8 to provide an intuitive comparison between JustHook and TempRMOT [5], where JustHook employs the encoder combination of ROPE Swin-T [34] + RoBERTa [35]. Here, (a) represents the results of TempRMOT [5], (b) represents the results of JustHook, GT denotes the ground truth, and  $T_1$ ,  $T_2$ , and  $T_3$  correspond to 3 sequentially sampled frames (which are not consecutive). In various scenarios, JustHook has demonstrated robust advantages, showing fewer error cases and lost cases compared to TempRMOT [5].

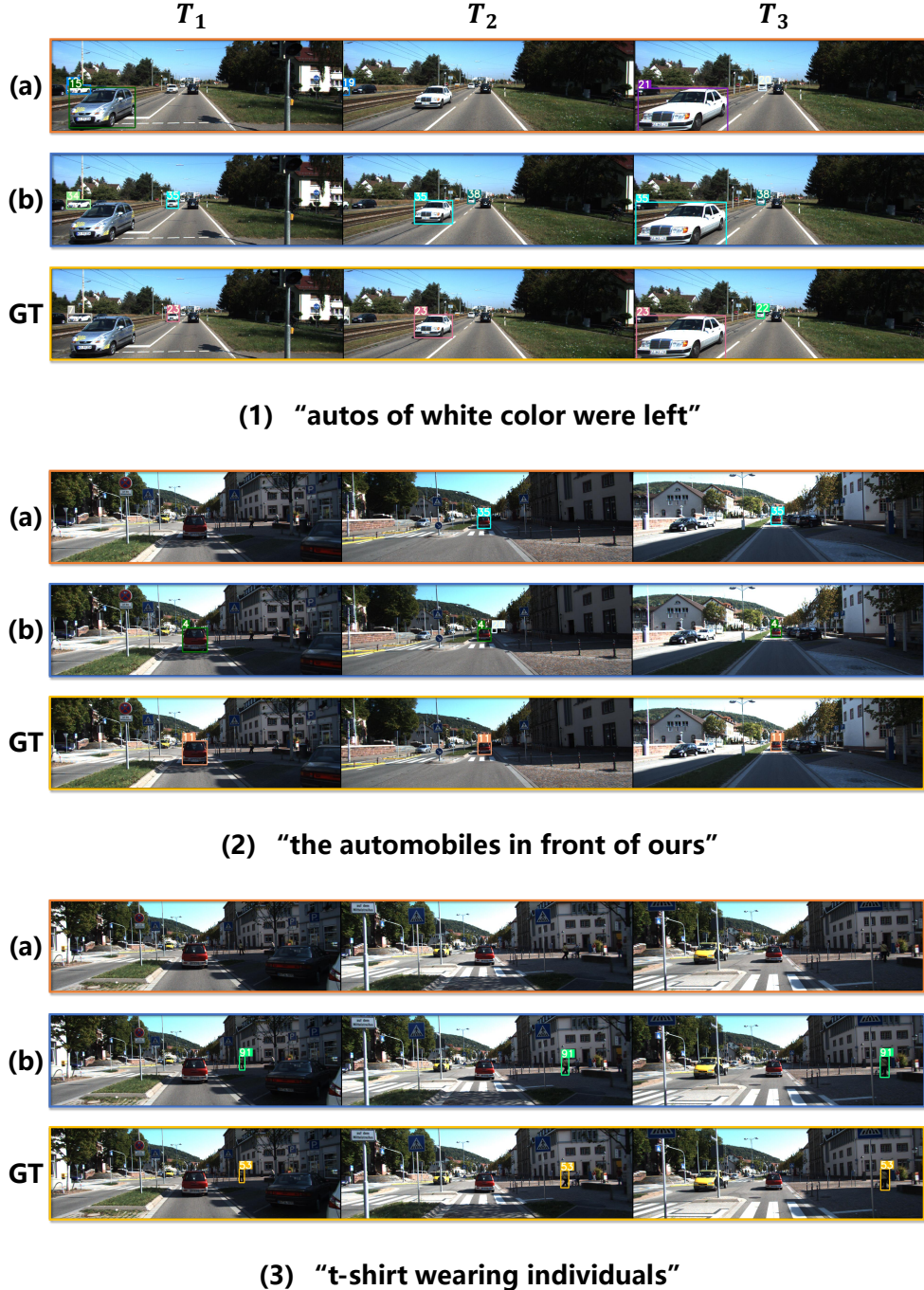


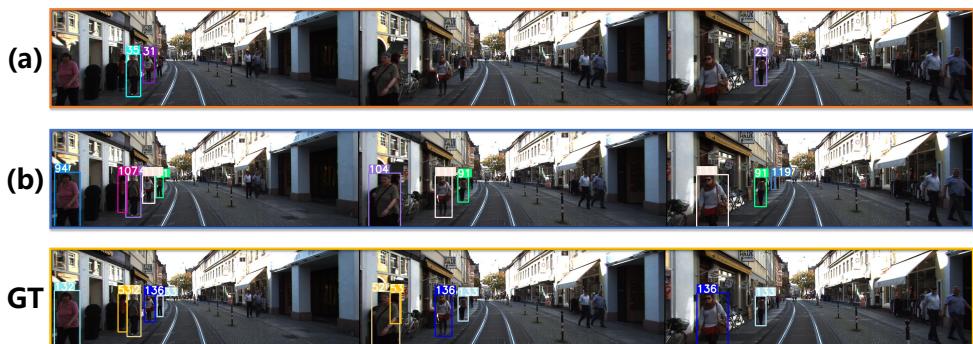
Figure 7: Visualization of some qualitative results (Part 2).



**(4) "those located on the right"**



**(5) "people on the left"**



**(6) "the ladies that are on the left side"**

Figure 8: Visualization of some qualitative results (Part 3).